## Online Supplement: A mechanistic model for protease sensor signal in atherosclerotic plaque

***Model Development.*** A mathematical model for the localization of fluorescence was developed for the three imaging agents. These agents circulate in the plasma and are taken up by fluid phase endocytosis.[1] The agents obtain their specificity by activation of the probe by proteases. Upon cleavage, adjacent auto-quenched fluorophores are separated, giving rise to an increase in fluorescence. In atherosclerosis, these enzymes are prevalent in high levels in plaque macrophages.[2] The process of signal gain and loss in the region of interest is a function of multiple steps. The agent must leave the plasma circulation, enter the plaque, get taken up by macrophage cells, be cleaved in the endosomes/lysosomes, and eventually leave the cell. Meanwhile, the agent is clearing from the plasma, lowering the amount taken up in the plaque. A reductionist approach was used to identify the important parameters for formulation of the model.

***Plasma Clearance.*** The luminal surface of the aorta is directly exposed to the plasma. Therefore, the plasma concentration of imaging agent is a critical factor in determining uptake. A single exponential or biexponential decay curve was used to fit plasma clearance data to describe this concentration. The biexponential behavior was derived from a two compartment model, where the drug is initially distributed in the plasma volume following a bolus intravenous injection, redistributes into normal tissues, and is cleared by various organs (e.g. liver, kidney, etc.). An equal fluorophore concentration was injected for each mouse, and assuming a 2 mL plasma volume for the mouse[3] and 5 nmol injection, the initial concentration in the plasma was 2.5 μM.

***Transport in Aortic Wall.*** While the luminal surface of the aorta is directly exposed to the plasma, agent must diffuse through the aortic wall in order to be taken up by macrophages. Macrophage and Cathepsin B are situated near the luminal surface of the vessel.[2] The intima-media thickness in the mouse aorta is approximately 55-60 microns[4] However, the 55 micron thickness measured under stress increases to 80 microns in the unloaded state.[5] At >500 beats per min,[5] the stretching of the aortic wall may cause a significant amount of convection over this distance, assuming irreversible (i.e. non-creeping) flow. It was assumed that this transport occurs only by diffusion, which is generally slower than convection. For a nanoparticle with an estimated[6] D = 2 $um^2/s$, it would take approximately 30 minutes to diffuse 60 microns. If the clearance from the plasma occurs at a much slower rate than 30 minutes, the agent should be able to reach this distance without a significant transport barrier. As it is diffusing between these tissues, it is being internalized by macrophage. To analyze the transport rate with consumption, a Thiele modulus was calculated. If this modulus is greater than one, it indicates consumption is faster than diffusion, in which case transport may still have to be considered.

The Thiele modulus for transport is the ratio of catabolism to the ratio of diffusion. Since pinocytosis internalizes a specific volume of fluid, this is a $1^{st}$ order reaction (i.e. higher concentrations will engulf a proportionally larger amount of material).

$$k_{pino} = \left(\frac{4uL \ \ \text{interstitium}}{hr \cdot 10^7 cells}\right)\left(\frac{hr}{3600s}\right)\left(\frac{(0.2)(4x10^8 cells)}{mL \ \ tissue}\right)\left(\frac{mL}{1000uL}\right)$$

$$k_{pino} = 8.9x10^{-6}/s$$

The Thiele modulus is then the ratio of reaction to diffusion:

$$\varphi^2 = \left(\frac{k_{pino}[Ab]_{\text{int}} R^2}{\varepsilon D[Ab]_{\text{int}}}\right)$$

$$\varphi^2 = \left(\frac{(8.9x10^{-6}/s)(60um)^2}{(0.1)(2um^2/s)}\right) = 0.16$$

Even with diffusion controlling transport, it does not appear that catabolism or clearance will be faster than access to the tissue. Therefore, transport through the aortic wall does not significantly affect the uptake. Several considerations are important, however. The rate of diffusion of these nanoparticles was not measured in a fibrous cap or in the presence of lipid deposits. Second, the distance in a mouse plaque can be significantly smaller than a human plaque.[7] Although the experimental data support the notion that there are no significant transport limitations in the plaque, the Thiele modulus is not well below one, thus, further consideration in other systems is required.

***Macrophage Pinocytosis.*** After the agent has transported from the plasma into the interstitium in the plaque, the local macrophages internalize it by pinocytosis. Activated macrophages internalize fluid faster than unactivated macrophage (e.g. 4-7 fold increase in pinocytosis[8]). Given that the macrophages in plaques are likely activated due to the local inflammatory environment, data from macrophage cell lines with faster pinocytosis rates were used. Three different primary cultures and 2 macrophage-like cell lines[9-13] estimated a rate of 4 uL/hr/$10^7$ cells for the fluid phase uptake. This was about 10-fold higher than lines with slower pinocytosis rates that appeared not to be activated.[14-16] Macrophage in general appear to have higher pinocytosis rates than other cell types (e.g. endothelial cells[17]) due to their phagocytic nature.

The density of these cells in the plaque also affect the overall activation of signal. The fraction of macrophage content in plaques ranges from 10-20% in humans with unstable disease.[18,19] For the mouse experiments, a 20% fraction was assumed. This fraction was multiplied by the cell density estimated at 4x10^8 cells/mL[20] to yield the concentration of macrophages.

***Sensor Activation.*** Once the agent is internalized, the polymer is cleaved in late endosomes and lysosomes.[1] If the rate of cleavage is fast compared to uptake and loss from the cell, then the fluorescence can be assumed to occur immediately and completely. In this case, the imaging signal would not be dependent on the rate of cleavage.

Almeida et al.[21] examined the cleavage rates of Cathepsin B on a quenched fluorescent peptide. The original peptide had a $k_{cat}$ of 0.45 /s and $k_{cat}/K_m$ of 75 /mM/s. We assumed that the reaction is 1st order (i.e. the substrate concentration is << $K_m$). The reaction rate is then:

$$\frac{d[S]}{dt} = \frac{-v_{\max}[S]}{K_m + [S]} = \frac{-k_{cat}[E][S]}{K_m + [S]}$$

$$\frac{d[S]}{dt} \approx -\left(\frac{k_{cat}[E]}{K_m}\right)[S]$$

The rate for substrate decay depends on $k_{cat}$/Km and the enzyme concentration. The enzyme concentration is more difficult to measure. It's concentrated in lysosomes, and the lower available volume increases the local concentration. For example, a single Cathepsin B enzyme in the typical volume of an endosome ($3.8 \times 10^{-13}$ μL)[17] yields a concentration of 4 μM and cleavage half life of 2.3 seconds. Even at a concentration of 50 nM in vitro,[22] the half life for cleavage is 3 min. Based on the 1st order catabolism rate in the Thiele modulus, the uptake half life is several hours. Given these ratios, we assumed that the cleavage rate does not strongly affect the accumulation of signal.

Experimental evidence supports the assumption of rapid cleavage, and fluorescence has been described after only 15 min incubation in cell culture.[1] While this was likely slowed by uptake, significant cleavage occurs in minutes, which is faster than the pinocytosis and signal loss rates (see below).

***Extracellular Activation.*** Proteases are primarily located in the lysosomes of macrophages, however, under certain circumstances, it can be expressed on the cell surface and shed into the surrounding interstitium.[23] To assess the impact this may have on total signal, the maximum contribution of interstitial fluorescence was estimated. Assuming 10% interstitial space for the imaging agent and instantaneous activation (maximum contribution), the fluorescence signal would be 10% of the concentration in the plasma. Since the above assumptions postulate that there are no transport barriers in the tissue itself, the interstitium is in equilibrium with the plasma. There will be no retention of unquenched fluorescence outside the cell (and any internalized 'activated' agent would be accounted for with the pinocytosis term). Under these assumptions, the extracellular fluorescence may have a small contribution, but it is always less than the intracellular fluorescence with the current model conditions. If transport in the plaque were slower, there could be significant accumulation of extracellular activated agent.

***Clearance from lysosomes.*** After the agent is activated in the lysosome, it will emit signal until it is lost by the cell (assuming no photobleaching). This rate is dependent on the retention of the cleaved product. For radioisotopes, the rate varies widely depending on the label. Iodine can leave the cell rather rapidly, but radiometals are often trapped for many hours to days inside the cell.[24]

To obtain an estimate for cellular retention in macrophages, the loss of signal of fluorescein labeled albumin was used.[25] The degraded portions likely diffuse back into the blood and are

cleared renally.[1] The same would hold true for any agent activated in the blood if the cleaved product is less than about 60 kDa.

Assuming rapid activation after internalization in the cells and no transport limitations from the plasma to the cells, the compartmental model is:

$$[I] \xrightarrow{k_{pinocytosis}} [A] \xrightarrow{k_{wash-out}}$$
$$\downarrow k_{clearance}$$

where [I] is the quenched (inactive) probe concentration and A is the fluorescent (active) probe concentration. The concentration can be converted into mol of probe using the wall volume of the aorta.[26]

Table S-1 Model Parameters

| Parameter | Value | References |
|---|---|---|
| $k_{clearance}$ | PS-5 = 3.50 x $10^{-5}$/s<br>PS-25 = 2.0 x $10^{-4}$/s (57%)<br>6.55 x $10^{-6}$/s (43%)<br>PS-40 = 1.01 x $10^{-5}$/s | Experiment |
| Dose $[PS]_0$ | 2.5 μM | Experiment |
| Plasma Volume | 2 mL | [3] |
| Pinocytosis Rate | 4 μL/hr/$10^7$ cells | [9-13] |
| $k_{pinocytosis}$ | 8.89 x $10^{-6}$ /s | Calculated |
| $k_{wash-out}$ | 1.28 x $10^{-5}$ /s | [25] |
| Macrophage fraction | 0.2 | [1, 8, 19] |
| Cell Density | 4 x $10^8$ cells/mL | [20] |
| Aorta Wall Volume | 38.1 $mm^3$ | [26] |

***Model Solution***

Single exponential plasma clearance:

Activated Probe: $$\frac{d[A]}{dt} = k_{pinocytosis}[I]_{plasma} - k_{wash-out}[A]$$

Plasma Concentration: $$[I]_{plasma} = [I]_{plasma,0}\exp\left(-k_{clearance}t\right)$$

where [A] is the activated (fluorescent) probe, [I] is the inactivated precursor, $K_{pinocytosis}$ is the net rate of probe uptake, $k_{wash\text{-}out}$ is the loss of fluorescence from the cells, $k_{clearance}$ is the rate of clearance from the plasma.

Solving the equation for [A] using an integrating factor:

$$\frac{d[A]}{dt} = k_{pinocytosis}[I]_{plasma,0}\exp\left(-k_{clearance}t\right) - k_{wash-out}[A]$$

$$[A] = \frac{k_{pinocytosis}[I]_{plasma,0}}{\left(k_{wash-out} - k_{clearance}\right)}\left[\exp\left(-k_{clearance}t\right) - \exp\left(-k_{wash-out}t\right)\right]$$

Maximum:

$$t_{\max} = \frac{\ln\left(\frac{k_{clearance}}{k_{wash-out}}\right)}{k_{clearance} - k_{wash-out}} \quad \text{and} \quad [A]_{\max} = \frac{k_{pinocytosis}[I]_{plasma,0}}{k_{clearance}}\left(\frac{k_{clearance}}{k_{wash-out}}\right)^{\left(\frac{k_{wash-out}}{k_{wash-out}-k_{clearance}}\right)}$$

Biexponential plasma clearance:

Activated Probe: $$\frac{d[A]}{dt} = k_{pinocytosis}[I]_{plasma} - k_{wash-out}[A]$$

Plasma Concentration: $$[I]_{plasma} = [I]_{plasma,0}\left[A\cdot\exp\left(-k_{\alpha}t\right) + B\cdot\exp\left(-k_{\beta}t\right)\right]$$

Solving the equation for [A] using an integrating factor:

$$\frac{d[A]}{dt} = k_{pinocytosis}[I]_{plasma,0}\left[A\cdot\exp\left(-k_{\alpha}t\right) + B\cdot\exp\left(-k_{\beta}t\right)\right] - k_{wash-out}[A]$$

$$[A] = k_{pinocytosis}[I]_{plasma,0}\left\{\begin{array}{l}\dfrac{A}{\left(k_{wash-out}-k_{\alpha}\right)}\left(\exp\left(-k_{\alpha}t\right)-\exp\left(-k_{wash-out}t\right)\right)+\\ \dfrac{B}{\left(k_{wash-out}-k_{\beta}\right)}\left(\exp\left(-k_{\beta}t\right)-\exp\left(-k_{wash-out}t\right)\right)\end{array}\right\}$$

Since the clearance is a biexponential, there is no explicit form for the time and concentration of maximum uptake. This has to be solved numerically.

***Model Optimization.*** The maximum uptake and time required to reach this value can be calculated explicitly for an exponential decay from the blood. With the current model, increases in uptake can be achieved with a higher uptake rate (increased pinocytosis, increased macrophage density, larger plaque size) or increased cellular retention. Many of the uptake parameters are dictated by the biology of the plaque, not the probe design, so decreasing the wash-out rate is more amenable to manipulation.

The effect of dose and plasma clearance is more complicated. An increased dose will provide more signal, but there will be an equal increase in the background. Slower plasma clearance will also yield a higher signal, but the waiting time to achieve this increases significantly, and there are diminishing returns on increased uptake. Using the model parameters, the effect of varying the plasma clearance half life versus the maximum uptake and waiting period between injection and imaging are plotted below for half lives spanning from 1 to 200 hrs. This large range covers from small, rapidly excreted agents to exceedingly long half lives similar to an IgG.

Fig. S-2

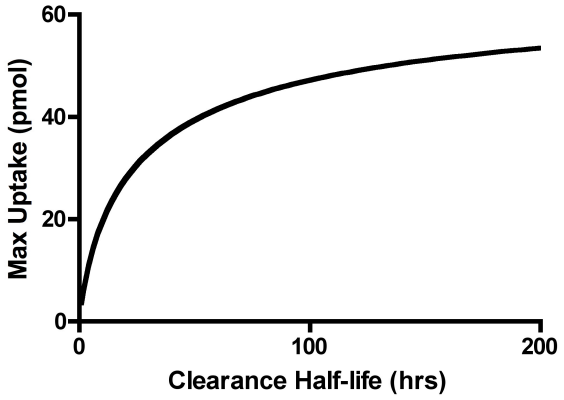


For maximum sensitivity, the highest uptake level is desired. However, due to loss of signal from the cells, there are diminishing returns with increased blood half life. The maximum achievable signal occurs when the blood clearance rate is much less than the cell wash-out rate, in which case:

$$[A]_{\max} = \frac{k_{pinocytosis}[I]_{plasma,0}}{k_{wash-out}}$$

At this point, the uptake is no longer a function of plasma clearance. Increasing the plasma half-life only increases the waiting time between injection and imaging. Looking at Fig. S-2, for a 24 hr waiting period, an 18 hr plasma half life is ideal. If a rapid imaging time is required, then a much faster plasma clearance rate would lower the optimal imaging time, although at the expense of sensitivity (maximum uptake).

**References:**


1. Weissleder, R., Tung, C. H., Mahmood, U. & Bogdanov, A. J. In vivo imaging of tumors with protease-activated near-infrared fluorescent probes. Nat Biotechnol 17, 375-378 (1999).
2. Chen, J. et al. In vivo imaging of proteolytic activity in atherosclerosis. Circulation 105, 2766-2771 (2002).
3. Kaliss, N. & Pressman, D. Plasma and blood volumes of mouse organs, as determined with radioactive iodoproteins. Proc Soc Exp Biol Med 75, 16-20 (1950).
4. Dileepan, K. N., Johnston, T. P., Li, Y., Tawfik, O. & Stechschulte, D. J. Deranged aortic intima-media thickness, plasma triglycerides and granulopoiesis in Sl/Sl(d) mice. Mediators Inflamm 13, 335-341 (2004).
5. Guo, X., Kono, Y., Mattrey, R. & Kassab, G. S. Morphometry and strain distribution of the C57BL/6 mouse aorta. Am J Physiol Heart Circ Physiol 283, H1829-37 (2002).
6. Boucher, Y., Pluen, A., Ramanujan, S., McKee, T. & Jain, R. K. Interstitial Diffusion of Macomolecules in Solid Tumors: Role of the Interstitial Matrix. Bioengineering Conference ASME 97-98 (2001).
7. Vengrenyuk, Y. et al. A hypothesis for vulnerable plaque rupture due to stress-induced debonding around cellular microcalcifications in thin fibrous caps. Proc Natl Acad Sci U S A 103, 14678-14683 (2006).
8. Swanson, J. A., Yirinec, B. D. & Silverstein, S. C. Phorbol esters and horseradish peroxidase stimulate pinocytosis and redirect the flow of pinocytosed fluid in macrophages. J Cell Biol 100, 851-859 (1985).
9. Burgert, H. G. & Thilo, L. Internalization and recycling of plasma membrane glycoconjugates during pinocytosis in the macrophage cell line, P388D1. Kinetic evidence for compartmentation of internalized membranes. Exp Cell Res 144, 127-142 (1983).
10. Walter, R. J., Berlin, R. D., Pfeiffer, J. R. & Oliver, J. M. Polarization of endocytosis and receptor topography on cultured macrophages. J Cell Biol 86, 199-211 (1980).
11. Besterman, J. M., Airhart, J. A., Low, R. B. & Rannels, D. E. Pinocytosis and intracellular degradation of exogenous protein: modulation by amino acids. J Cell Biol 96, 1586-1591 (1983).
12. Besterman, J. M., Airhart, J. A., Woodworth, R. C. & Low, R. B. Exocytosis of pinocytosed fluid in cultured cells: kinetic evidence for rapid turnover and compartmentation. J Cell Biol 91, 716-727 (1981).
13. Duncan, R., Pratten, M. K., Cable, H. C., Ringsdorf, H. & Lloyd, J. B. Effect of molecular size of 125I-labelled poly(vinylpyrrolidone) on its pinocytosis by rat visceral yolk sacs and rat peritoneal macrophages. Biochem J 196, 49-55 (1981).
14. Pratten, M. K., Cable, H. C., Ringsdorf, H. & Lloyd, J. B. Adsorptive pinocytosis of polycationic copolymers of vinylpyrrolidone with vinylamine by rat yolk sac and rat peritoneal macrophage. Biochim Biophys Acta 719, 424-430 (1982).

15. Pratten, M. K. & Lloyd, J. B. Effect of suramin on pinocytosis by resident rat peritoneal macrophages: an analysis using four different substrates. Chem Biol Interact 47, 79-86 (1983).
16. Selby, D. M. et al. Antigen-presenting cell lines internalize peptide antigens via fluid-phase endocytosis. Cell Immunol 163, 47-54 (1995).
17. Marsh, M. & Helenius, A. Adsorptive endocytosis of Semliki Forest virus. J Mol Biol 142, 439-454 (1980).
18. Moreno, P. R. et al. Macrophage infiltration in acute coronary syndromes. Implications for plaque rupture. Circulation 90, 775-778 (1994).
19. Tearney, G. J. et al. Quantification of macrophage content in atherosclerotic plaques by optical coherence tomography. Circulation 107, 113-119 (2003).
20. Alkhatib, B. et al. Antidonor humoral transfer induces transplant arteriosclerosis in aortic and cardiac graft models in rats. J Thorac Cardiovasc Surg 133, 791-797 (2007).
21. Almeida, P. C. et al. Hydrolysis by cathepsin B of fluorescent peptides derived from human prorenin. Hypertension 35, 1278-1283 (2000).
22. Premzl, A., Zavasnik-Bergant, V., Turk, V. & Kos, J. Intracellular and extracellular cathepsin B facilitate invasion of MCF-10A neoT cells through reconstituted extracellular matrix in vitro. Exp Cell Res 283, 206-214 (2003).
23. Gacko, M., Chyczewski, L. & Chrostek, L. Distribution, activity and concentration of cathepsin B and cystatin C in the wall of aortic aneurysm. Pol J Pathol 50, 83-86 (1999).
24. Ferl, G. Z., Kenanova, V., Wu, A. M. & DiStefano, J. J. r. A two-tiered physiologically based model for dually labeled single-chain Fv-Fc antibody fragments. Mol Cancer Ther 5, 1550-1558 (2006).
25. Maxwell, J. L., Terracio, L., Borg, T. K., Baynes, J. W. & Thorpe, S. R. A fluorescent residualizing label for studies on protein uptake and catabolism in vivo and in vitro. Biochem J 267, 155-162 (1990).
26. Trogan, E. et al. Serial studies of mouse atherosclerosis by in vivo magnetic resonance imaging detect lesion regression after correction of dyslipidemia. Arterioscler Thromb Vasc Biol 24, 1714-1719 (2004).